INTERFACE SCIENCE 9, 93–104, 2001

Stress-Assisted Reaction at a Solid-Fluid Interface

J. LIANG AND Z. SUO
Mechanical Engineering Department and Princeton Materials Institute, Princeton University, Princeton, NJ 08544, USA
suo@princeton.edu

Abstract. On the interface between a solid and a fluid, a reaction can occur in which atoms either leave the solid to join the fluid, or leave the fluid to join the solid. If the solid is in addition subject to a mechanical load, two outcomes may be expected. The reaction may proceed uniformly, so that the interface remains flat as the solid recedes or extends. Alternatively, the reaction may cause the interface to roughen and develop sharp cracks, leading to fracture. This paper reviews the current understanding of the subject. The solid-fluid is a thermodynamic system: the solid is in elastic equilibrium with the mechanical load, but not in chemical equilibrium with the fluid. Thermodynamic forces that drive the interfacial reaction include chemical energy difference between the solid and the fluid, elastic energy stored in the solid, and interfacial energy. The reaction is taken to be thermally activated. A kinetic law is adopted in which the stress affects both the activation energy and the driving force of the interface reaction. A linear perturbation analysis identifies the stability condition, which differs substantially from the well known stability condition based on the driving force alone. Large perturbations are examined by assuming that the interface varies as a family of cycloids, from slight waviness to sharp cracks. An analytic elasticity solution is used to compute the stress field in the solid, and a variational method to evolve the shape of the interface.

Keywords: interface reaction, interface instability, stress effect, elasticity, kinetics

1. Introduction

The question of surface instability of stressed solids arises in many technical situations, including growth of thin films, delayed fracture of optical fibers, and etching of microelectromechanical components. In such a situation, a solid is immersed in a fluid (gas or liquid). On the interface between the solid and the fluid, a reaction occurs in which the solid recedes by losing mass to the fluid. If the fluid contains the components of the solid, the solid can also extend by gaining mass from the liquid. For example, when the solid extends by gaining atoms from its own vapor in the surrounding, atoms must diffuse in the vapor, react on the interface, and become part of the solid structure. Either diffusion in the vapor or reaction on the interface may be the rate-limiting step. In this paper, the reaction on the interface is taken to be the rate-limiting step. The solid may grow facets when the reaction is anisotropic, or grow pits when the interface is inhomogeneous. These effects are assumed to be negligible in the system to be considered. Ideal examples include pure silica glass and amorphous metals.

Mullins [1] considered such an idealized solid, under no mechanical load, in contact with its own vapor. The pressure of the vapor is held in equilibrium with the solid when the interface is flat. If the interface is perturbed into a sinusoidal shape, the system deviates from equilibrium: the interfacial energy causes evaporation at crests, and condensation at troughs. Over time the perturbation amplitude decays, and the interface becomes flat. One can also consider a vapor not in equilibrium with the flat solid. Say the pressure of the vapor is held far below the equilibrium value, and the solid evaporates on the entire interface. For a wavy interface, the interfacial energy biases the evaporation rate, so that the solid evaporates faster at crests than at troughs. Over time the perturbation amplitude decays, although the interface keeps moving. That is, under no mechanical load, the interfacial energy stabilizes the flat interface.

This stability is affected when the solid is subject to a mechanical load. Consider a stress applied to the solid in the direction nominally in the plane of the interface. Srolovitz [2] added the elastic energy density to the driving force of evaporation. He assumed that evaporation rate is proportional to the driving force, but the proportionality constant is unaffected by the stress. He showed that a sinusoidal interface is stable if the wavelength is short, but unstable if the wavelength is long. Because the stress enters through the elastic energy density, which is quadratic in the stress, his model predicts identical behaviors for solids under tension and compression. Similar conclusions have been reached by Asaro and Tiller [3], Grinfel'd [4] and others. Chiu and Gao [5] further showed that the wave amplitude can grow all the way to sharp cracks. Kim et al. [6] developed a stress measurement technique on the basis of this model. They immersed a stressed solid in an etchant, and scanned the solid surface at various times by using an atomic force microscope. They determined stress state by comparing the change in the surface profile with that predicted by the model.

The assumption that the stress affects only the driving force is inadequate. It has long been understood that stress can affect the activation energy of the reaction as well. On the basis of such a stress-dependent kinetic law, Hillig and Charles [7] and Chuang and Fuller [8] developed a theory of delayed fracture. Aziz et al. [9] studied the motion of the interface between crystalline and amorphous silicon. At elevated temperatures, the crystalline silicon grew at the expense of the amorphous silicon. The growth velocity was measured as a function of the stress applied in the plane of the interface, and was found to linearly increase with the stress. The data were interpreted as the effect of the stress on the activation energy.

This linear effect of stress on the reaction velocity can completely alter the interface stability. Barvosa-Carter et al. [10] described a numerical simulation and predicted that the interface is stable under tension, and roughens under compression. They confirmed the latter prediction experimentally. These predictions are qualitatively different from that of the Srolovitz model [2]. Furthermore, the critical wavelength of unstable perturbation is about one order of magnitude smaller than that predicted by the Srolovitz model.

In a different experiment, with a crystalline silicon immersed in an etchant, Shreter et al. [11] observed that the silicon surface developed crack-like defects under compression, but remained flat under tension. As will become evident, these experimental observations are consistent with the notion that the etching rate varies linearly with stress, provided the etching rate *decreases* with the increasing stress. However, no direct measurement of the stress effect on the etching rate is known to us.

The plan of this paper is as follows. First, we will formulate stress assisted interfacial reaction within the framework of partial-equilibrium thermodynamics, adopting a kinetic law in which stress affects both driving force and activation energy. Second, we will study in detail the results of the linear perturbation analysis. Third, we will study large perturbation by assuming that the interface evolve as a family of cycloids according to a variational statement. These issues are of general character; we will review the theoretical development in some detail. Suo [12, 13] has reviewed the same approach to several other phenomena.

Figure 1 illustrates the problem to be analyzed in this paper. A semi-infinite solid is under an applied stress, S, nominally parallel to the interface. For simplicity, we will consider a plane stress problem. The interface initially is sinusoidal, with the amplitude q much smaller than the wavelength λ. The solid is isotropic and elastic with Young's modulus E. The stress at the interface, σ, acts in the direction tangential to the interface. When the interface is flat, the stress in the solid is uniform, and $\sigma = S$. When the interface is not flat, the stress in the solid is nonuniform, and σ has to be determined by solving the elasticity boundary value problem. The solid is in contact with a fluid; the interface moves when the solid gains or loses mass.

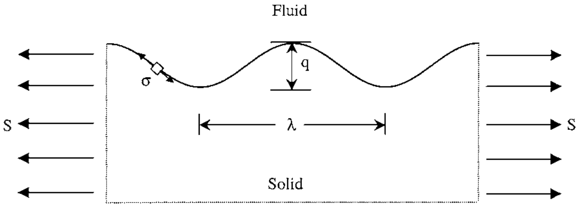

Figure 1. The geometry of the problem. A solid is in contact with a fluid and subject to a stress. A reaction occurs on the interface, causing the interface to change shape. The initial interface shape is sinusoidal, with wavelength λ and amplitude q.

2. Partial-Equilibrium Thermodynamics

Because the solid and the fluid are not in equilibrium, when the solid gains atoms from or loses atoms to the fluid, the free energy changes. The system can be separated into two parts: the bulk and the interface. First consider the bulk free energy change. Let g be the chemical free energy increase associated with the solid gaining a unit volume at the expense of the fluid. The fluid mass is taken to be so large that its chemical potential remains constant at all time, namely, g is a constant. If V is the total volume gained by the solid, the total chemical free energy increase is $U_\mathrm{C} = gV$. When the solid is subject to a stress field, the elastic energy is the elastic energy density w integrated over the entire volume of the solid, $U_\mathrm{E} = \int w dV$. Next consider the interfacial energy. Let γ be the excess energy per unit interface area. Assume that γ is independent of the strain, namely, neglect the effect of the surface stress. If A is the area of the interface, the interfacial energy is $U_\mathrm{I} = \gamma A$. The loading device, which applies the stress S remotely to the solid, is taken to be perfectly rigid, and does no additional work as the solid gains or loses mass. The total free energy is the sum

$$G = U_\mathrm{C} + U_\mathrm{E} + U_\mathrm{I} = gV + \int w dV + \gamma A. \quad (1)$$

In this paper, the volume and the area are those in the reference state, i.e., the unstrained solid. The reaction proceeds in the direction that reduces this free energy. The three terms have different effects on interface motion, as qualitatively noted below.

The chemical free energy changes when the solid changes volume. When $g > 0$, the chemical energy reduces if the solid loses mass to the fluid. Conversely, when $g < 0$, the chemical energy reduces if the solid gains mass from the fluid. By itself the chemical free energy does not affect the interface shape.

The elastic energy reduces when either the solid loses mass or the interface roughens. We have assumed that the solid is semi-infinite. We further assume that atoms freshly grown on the solid acquire the local elastic strain, namely, no stress-relieving defects form. Imagine two artificial situations. First, the solid changes volume, and the interface translates without changing the shape. The stress field is self-similar as the interface translates, and the elastic energy reduces as the solid loses mass to the fluid. Second, the interface changes shape, but the volume of the solid remains invariant. The solid with a wavy interface has lower total elastic energy than the solid has the flat interface. Consequently, the elastic energy tends to destabilize the flat interface.

The interfacial energy changes when the interface changes shape. The interfacial energy density γ is always positive, so that the interfacial energy reduces when the interface reduces area, and is minimal when the interface is flat. Consequently, the interfacial energy tends to stabilize the flat interface.

As illustrated in Fig. 2, the solid-fluid as a thermodynamic system can vary by two processes: (1) the solid deforms elastically, and (2) the solid gains or loses mass on the interface. In reality the two processes occur simultaneously, but it is convenient to analyze them separately. Let u_i be the elastic displacement field in the solid. The elastic energy density is a quadratic function of the strain (i.e., the displacement gradient), $w(u_{i,j})$. The stress tensor σ_{ij} relates to the energy density function as $\sigma_{ij} = \partial w / \partial u_{i,j}$. Let dA be a differential element of the interface. When the element moves in the normal direction by a small distance δr_n, the solid extends by volume $\delta r_n dA$. The

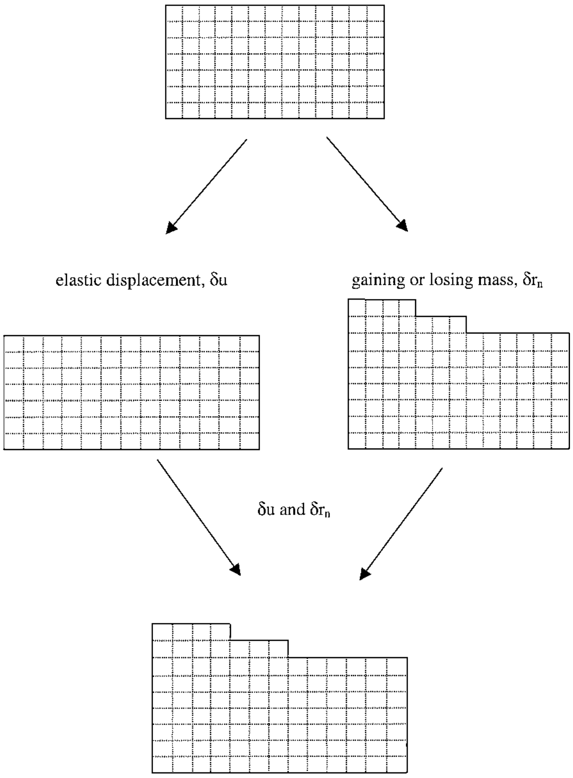

Figure 2. The system can vary by two processes. The solid deforms elastically, or gains/loses mass.

magnitude of the movement δr_n can vary over the interface. We adopt the sign convention that $\delta r_n > 0$ when the solid gains mass, and $\delta r_n < 0$ when the solid loses mass.

A small variation of the thermodynamic system is represented by a variation in the displacement field, δu_i, and a variation in the interface position, δr_n. Associated with these variations, the free energy (1) varies by

$$\delta G = \int \frac{\partial w}{\partial u_{i,j}} \delta u_{i,j} dV + \int (g + w + \gamma K) \delta r_n dA. \tag{2}$$

Derivations of this expression can be found in, e.g., [12, 14]. We adopt the convention of summation over the repeated index. The first integral results from the variation in the displacement field δu_i, and extends over the solid volume. The second integral results form adding mass to or removing mass from the solid δr_n, and extends over the interface area. The curvature of the interface, K, is taken to be positive at points where the solid is convex. The elastic energy density w in the second integral is evaluated at the interface, related to the stress at the interface σ as $w = \sigma^2/2E$.

The system attains thermodynamic equilibrium when $\delta G = 0$ for arbitrary variations δu_i and δr_n. However, we are mainly interested in partial equilibrium, in which the free energy variation associated with the displacement variation vanishes, but that associated with the reaction does not. That is, the reaction rate is so slow that the solid is in elastic equilibrium with the applied load at all time. Consequently, the first integral in (2) vanishes for any small variation in the displacement field:

$$\int \frac{\partial w}{\partial u_{i,j}} \delta u_{i,j} dV = 0. \tag{3}$$

This is a variational statement of the elasticity problem [15]. Recall that $\sigma_{ij} = \partial w / \partial u_{i,j}$. Use the divergence theorem to express the above integral in terms of the variation in the displacement, yielding

$$\int \sigma_{ij} n_j \delta u_i dA - \int \sigma_{ij,j} \delta u_i dV = 0, \tag{3a}$$

where n_i is the unit vector normal to the solid surface. The first integral extends to the entire surface of the solid, and corresponds to the boundary conditions of the elasticity problem. On the fluid-solid interface, the elastic displacement is unconstrained, so that δu_i can take arbitrary value, and (3a) implies that $\sigma_{ij} n_j = 0$ on the interface, which is the traction-free boundary condition. On the solid surface where the stress is applied by a prescribed displacement, $\delta u_i = 0$, so that the surface integral vanishes. The second integral in (3a) extends to the volume of the solid, and corresponds to the equilibrium equations in the solid, $\sigma_{ij,j} = 0$.

The solid and the fluid are not in chemical equilibrium with each other. Consequently, the second integral in (2) does not vanish. When the interface is not flat, the reaction rate is nonuniform on the interface. A common procedure to formulate the kinetic law is as follows. Define the driving force F for the reaction at each material point on the interface as the free energy reduction when the solid gains a unit volume. Thus,

$$\int F \delta r_n dA = -\delta G. \tag{4}$$

The integration is over the entire interface area. Equation (4) requires that the solid is in elastic equilibrium with the mechanical load. It is the variational statement of the interfacial reaction. One can base numerical calculation on this statement, as will be done later.

Alternatively, one can obtain an explicit expression for the driving force. A comparison between (2) and (4) gives

$$F = -g - w - \gamma K. \tag{5}$$

This expression gives the driving force at any small element of the interface, pointing in the direction of the reaction. When $F > 0$, the solid gains mass at the interface element to reduce the total free energy. When $F < 0$, the solid loses mass at the interface element to reduce the total free energy. One can examine the effect of the three terms on the interface stability again using the driving force. For the wavy interface in Fig. 1, g is constant and does not affect the interface shape. The elastic energy density w is larger at the troughs than at crests, and therefore destabilizes the interface. The curvature is positive at the crests and negative at the troughs, so that the interfacial energy tends to stabilize the interface.

Let v_n be the reaction rate, namely, $v_n dA$ is the volume of the solid gained at the element dA per unit time. Consistent with the sign convention of δr_n, $v_n > 0$ when the solid gains mass, and $v_n < 0$ when the solid loses mass. A kinetic law relates the reaction rate v_n to the driving force F. Information on kinetic laws is very limited. Various functional forms have been proposed on the basis of the transition state theory [7, 9, 10, 16]. The form of the kinetic law will affect the results, but not the analysis procedure, that are described in the following sections. In this paper, to be definite, we adopt the following form:

$$v_n = v_0 \exp\left(\frac{-Q + \sigma\varepsilon^*\Omega}{kT}\right) \sinh\left(\frac{F\Omega}{2kT}\right). \tag{6}$$

The reaction is thermally activated, with Q being the activation energy in the absence of the stress, k Boltsmann's constant, T the temperature, v_0 the pre-exponential factor, ε^* the activation strain, and Ω the volume per atom. Under the stress σ, the transitional complex is affected, and the activation energy changes to $Q - \sigma\varepsilon^*\Omega$.

In this form, the stress affects both the driving force and the activation energy. When the activation strain is negligible, $\varepsilon^* = 0$, and the driving force is small, $F\Omega/2kT \ll 1$, the above law reduces to $v_n = MF$, where M is a constant. This linear kinetic law was adopted by Srolovitz [2] in his analysis.

The effect of the activation strain can be readily understood as follows. When $\varepsilon^* > 0$, a tensile stress σ lower the activation energy and increases the reaction rate. Further assume that the solid is far from equilibrium and gains mass on the interface. The conditions are satisfied by the growth of crystalline silicon at the expense of amorphous silicon [10]. Treat the amorphous silicon at elevated temperatures as a viscous liquid. When the solid (i.e., the crystalline silicon) is under tension (Fig. 3(a)), the stress is larger at the troughs than at crests, so that the solid gains mass faster at troughs than at the crests, and the wave amplitude decays over time. Conversely, when the solid is under compression (Fig. 3(b)), the stress is more negative at the troughs than at crests, so that the solid gains mass slower at troughs than at the crests, and the wave amplitude grows over time.

In the etching experiments described by Shreter et al. [11], the crystalline silicon loses mass to the fluid. The experiments showed that the interface is stable when the solid is under tension, but unstable when the solid is under compression. To be compatible with the present theory, the activation strain of this reaction must be negative, $\varepsilon^* < 0$. No information, however, is available to us regarding the sign of the activation strain in this reaction.

The applied stress affects reaction rate through both the driving force and the activation energy. A quantitative analysis is needed to study their interplay. The above considerations prescribe a procedure to evolve the interface shape. At a given time, the interface shape is known, and the elastic field in the solid is determined by solving the boundary value problem. Equation (5) then gives the driving force for reaction, and Eq. (6) updates the interface shape for a small time step. Repeat the procedure for the subsequent time steps. The time evolution is considered in the following two sections.

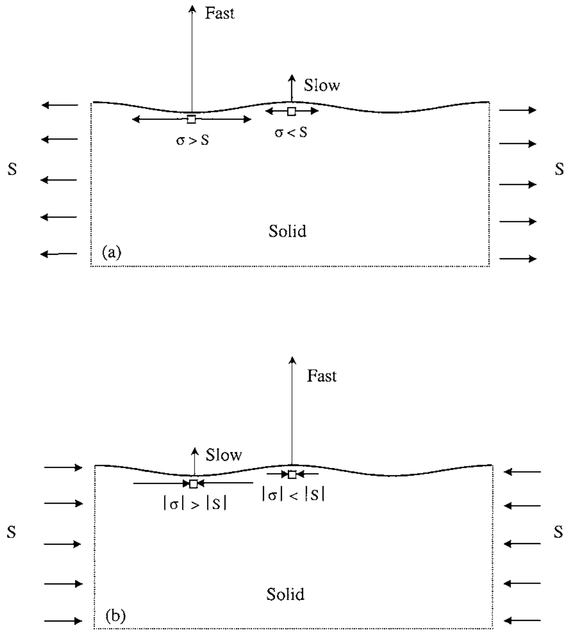

Figure 3. Assume that the solid gains mass ($F_0 > 0$) and that the activation strain is positive ($\varepsilon^* > 0$). (a) When the solid is under tension, the stress at crests is smaller than at troughs, so that the solid gains mass slower at the crests than at the troughs, and the perturbation amplitude decays. (b) When the solid is under compression, the stress at crests is less negative than at troughs, so that the solid gains mass faster at the crests than at the troughs, and the perturbation amplitude amplifies.

3. Small Perturbation

Yu and Suo [16] has performed a fairly general small perturbation analysis. Here we specialize the analysis for this discussion. The interface is taken to be nearly flat with a sinusoidal perturbation (Fig. 1). Let $H(x, t)$ be the position of the interface above the x-axis at time t, written as

$$H(x, t) = H_0(t) + q(t)\cos(\omega x), \tag{7}$$

where $H_0(t)$ is the average height, $\omega = 2\pi/\lambda$ the perturbation wavenumber, and $q(t)$ the perturbation amplitude. Both the average height H_0 and the perturbation amplitude q vary with time. The following analysis determines their time evolution.

The perturbation is small in that $q/\lambda \ll 1$. In the linear perturbation analysis, various quantities are computed to the first order in q. The interface velocity relates to the interface position $H(x,t)$ as $v_n = (\partial H/\partial t)[1 + (\partial H/\partial x)^2]^{-1/2}$. Thus, to the first order in q, we have

$$v_n = \frac{dH_0}{dt} + \frac{dq}{dt}\cos(\omega x). \tag{8}$$

As expected, dH_0/dt is the average interface velocity, and dq/dt is the magnitude of the velocity fluctuation. The curvature is given by $K = -(\partial^2 H/\partial x^2)[1 + (\partial H/\partial x)^2]^{-3/2}$, namely,

$$K = \omega^2 q\cos(\omega x). \tag{9}$$

The curvature is positive at crests and negative at troughs. An elasticity boundary value problem determines the stress at the interface [3]:

$$\sigma = S[1 - 2\omega q\cos(\omega x)]. \tag{10}$$

The magnitude of the stress σ is below the magnitude of S at crests, and above the magnitude of S at troughs. The elastic energy density at the interface is given by

$$w = \frac{S^2}{2E}[1 - 4\omega q\cos(\omega x)]. \tag{11}$$

Expand the kinetic law (6) into the Taylor series to the first power in q, and we obtain that

$$v_n = C + Bq\cos(\omega x), \tag{12}$$

with

$$\begin{aligned} B &= \frac{\Omega v_0}{2kT}\exp\left(\frac{-Q + S\varepsilon^*\Omega}{kT}\right)\cosh\left(\frac{F_0\Omega}{2kT}\right) \\ &\quad\times\left\{\left[\frac{2S^2}{E} - 4S\varepsilon^*\tanh\left(\frac{F_0\Omega}{2kT}\right)\right]\omega - \gamma\omega^2\right\}, \end{aligned} \tag{13}$$

$$C = v_0\exp\left(\frac{-Q + S\varepsilon^*\Omega}{kT}\right)\sinh\left(\frac{F_0\Omega}{2kT}\right), \tag{14}$$

and $F_0 = -g - S^2/2E$.

Now we compare (8) and (12). From the zeroth order terms in q we obtain the average interface velocity, $dH_0/dt = C$. One can also obtain this result by simply assuming that the interface is perfectly flat. Because the average interface velocity dH_0/dt can be measured as a function of the applied stress S, Eq. (14) can be used to fit the experimental data to determine the activation strain, as was done by Aziz et al. [9].

From the first order terms in q in (8) and (12) we obtain that

$$\frac{dq}{dt} = Bq. \tag{15}$$

This ordinary differential equation determines the perturbation amplitude as a function of time:

$$q(t) = q(0)\exp(Bt), \tag{16}$$

where $q(0)$ is the perturbation amplitude at time $t = 0$. Equation (16) shows that when $B > 0$, the perturbation amplitude grows exponentially with time, and the interface is unstable. When $B < 0$, the perturbation amplitude decays exponentially with time, and the interface is stable.

Equation (13) gives the characteristic number B. The sign of B is determined by the quantity in { }. Various terms affect the interface stability as follows. The interfacial energy stabilizes the flat interface. The elastic energy density $S^2/2E$ appears in two places inside { }. Typically, the chemical free energy density is much larger than the elastic energy density, $|g| \gg S^2/2E$, so that we adopt the approximation $F_0 \approx -g$. Equation (13) shows that the elastic energy density tends to destabilize the flat interface. Now look at the term in { } involving the activation strain, E^*. The sign of this term depends on the signs of S, E^* and F_0. The activation strain tends to stabilize the interface when $SE^*\ F_0 > 0$, and destabilize the interface if $SE^*\ F_0 < 0$. The physical interpretion of these conclusions have been given in the previous section.

We next examine the effect of the wavenumber, ω. Note that B is a quadratic function of ω. The interface is stable against small-amplitude perturbation of *all* wavenumbers if the quantity in front of the linear term of ω in (13) is negative, namely,

$$2 - 4\left(\frac{E\varepsilon^*}{S}\right)\tanh\left(\frac{F_0\Omega}{2kT}\right) < 0. \tag{17}$$

This inequality corresponds to the shaded regions in Fig. 4. The experiment of Barvosa-Carter et al. [10] on amorphous-crystalline silicon interface is represented by a point in the region $S/E\varepsilon^* < 0$ and $F_0\Omega/kT > 0$.

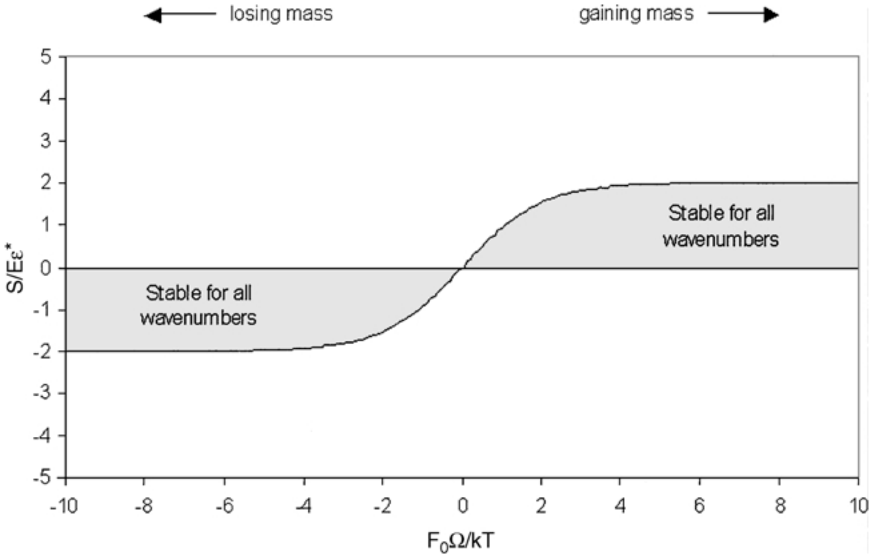

Figure 4. Stability map. A given experiment corresponds to a point on the plane of $S/E\varepsilon^*$ and $F_0\Omega/kT$. The shaded regions correspond to systems stable against perturbations of small amplitude of *all* wavenumbers. The unshaded regions correspond to systems unstable under perturbation of small amplitude of *some* wavenumbers.

Their experiments showed that $\varepsilon^* > 0$, and that the interface under compression is unstable. The experiments of Shreter et al. [11] are represented by two points on the map (assuming $\varepsilon^* < 0$ and $F_0 < 0$), one is under tension (stable) the other under compression (unstable). The paucity of the available experimental data left the map largely unexplored.

When the quantity in (17) is positive, $B > 0$ for small ω, and $B < 0$ for large ω. That is, the flat interface is unstable against perturbations of small wavenumbers, but stable against perturbations of large wavenumbers. The critical wavenumber at which $B = 0$ is given by

$$l\omega_c = 2 - 4\left(\frac{E\varepsilon^*}{S}\right)\tanh\left(\frac{F_0\Omega}{2kT}\right). \tag{18}$$

A length scale $l = \gamma E/S^2$ is used to scale the wavenumber. This equation is plotted for $l\omega_c = \pi/3$ in Fig. 5(a), and for $l\omega_c = 3$ in Fig. 5(b). If a pair of parameters $S/E\varepsilon^*$ and $F_0\Omega/kT$ falls in a shaded region, a perturbation of a wavenumber larger than ω_c will decay.

Figure 6 plots B as a function of the wavenumber in a dimensionless form, assuming that $F_0\Omega/kT = -1$. The figure compares the cases with and without the activation strain. The curve for $E\varepsilon^*/S = 0$ represents the case where the activation strain is negligible. The curve is the same as that given by Srolovitz [2], who assumed that the stress only affects the driving force but not the activation energy. A more representative order of magnitude is $E\varepsilon^*/S = 10$. The two curves differ substantially. In either case, the quantity B is maximal when the wavenumber is $\omega = \omega_c/2$. The perturbation of this wavenumber grows faster than perturbations of other wavenumbers.

4. Large Perturbation

The above discussions are based on the small perturbation analysis, where the perturbation amplitude is assumed to be much smaller than the wavelength. We would like to ascertain that when the interface is linearly unstable, cracks can nucleate on the interface. That is, we would like to study the behavior of the interface with large perturbations. Two issues need be addressed: the elasticity field in a solid bounded by an interface that is not flat, and the time evolution of such an interface. Following Chiu and Gao [5], we will assume that the interface evolves as a family of cycloids. The elasticity field of a semi-infinite solid bounded by a cycloid is available in an analytical form. The cycloids can represent, in two limits, both a flat interface and an interface with sharp cracks. A difficulty exists if one uses the rate Eq. (6) directly to evolve the interface shape. After the first few time steps, the interface is no longer a cycloid. It is difficult to obtain the elasticity solution for an arbitrary interface shape. To circumvent this difficulty, we will evolve the shape of the interface

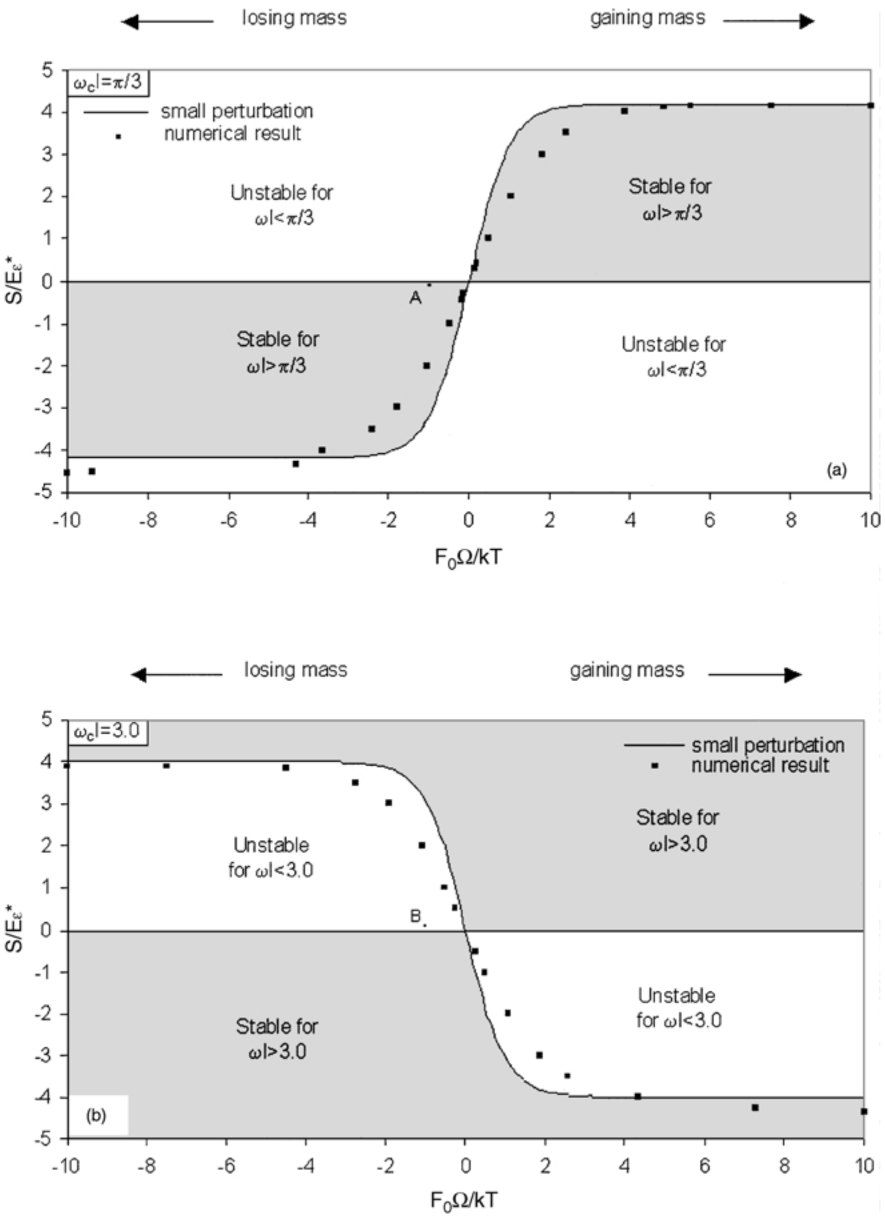

Figure 5. Level plots of the critical wavenumber ω_c on the plane spanned by the parameters $S/E\varepsilon^*$ and $F_0\Omega/kT$. (a) $l\omega_c = \pi/3$. (b) $l\omega_c = 3$.

according to a variational approach developed by Suo and Yu [17]. When the interface is represented by a family of curves, such as cycloids, an artificial constraint is introduced into the problem. More realistic solutions can only be obtained by representing the interface by a larger family of curves. Such an extension has been carried out by Yu and Suo [18] assuming the linear kinetic law. In this paper, to illustrate the procedure without excessive computation, we will restrict the interface to be a family of cycloids.

A cycloid is the trajectory of a point fixed on a circular disc that rolls without slipping on a flat surface. Take the x-axis to be parallel and the y-axis to be perpendicular to the surface. Consider a disc of radius R, with a point fixed at a distance αR from the disc center. The disc center is at a distance βR above the x-axis. When the disc rolls by an angle θ, the point fixed on the disc moves to the coordinates

$$x = (\theta + \alpha \sin\theta)R, \quad y = (\beta + \alpha \cos\theta)R. \tag{19}$$

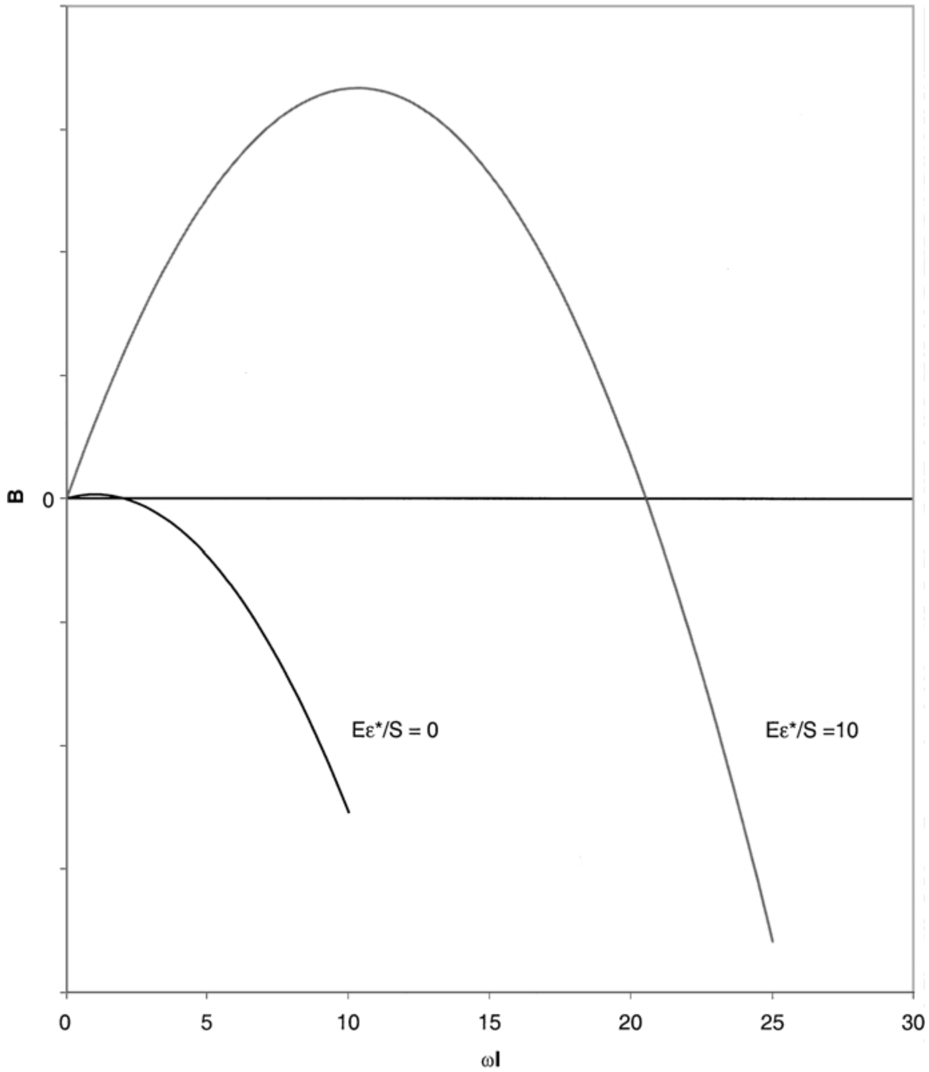

Figure 6. The characteristic number B as a function of the wavenumber. The scale of the vertical axis is arbitrary. Fix $F_0\omega/kT = -1$. The effect of the activation strain is illustrated by two curves for $E'\varepsilon^*/S = 0$, and $E'\varepsilon^*/S = 10$.

When θ changes from $-\infty$ to $+\infty$, Eq. (19) represents a cycloid curve. The curve is periodic, with the wavelength $\lambda = 2\pi R$. The parameter β describes the average height of the curve. As illustrated in Fig. 7, α describes the shape of the curve. When $\alpha = 0$, the curve is a straight line. When $\alpha = 1$, the curve forms periodic cusps, and cracks are said to have nucleated. When $0 < \alpha < 1$, the curve is undulating but smooth. In the following analysis, we will assume that R is fixed, but α and β can vary with time. Consequently, α and β are the generalized coordinates of this thermodynamic system.

The reference energy state is a flat surface lying on the x-axis ($\alpha = \beta = 0$). The solid is infinitely deep beneath its surface. We will compute energy per unit thickness per period. The excess chemical free energy is g times the area between the cycloid and the x-axis, given by

$$U_{\mathrm{C}} = \pi g R^2(2\beta + \alpha^2). \tag{20}$$

The difference in the elastic energy between the evolved and the flat body is given by

$$U_{\mathrm{E}} = \frac{\pi R^2 S^2}{2E'}(2\beta - \alpha^2). \tag{21}$$

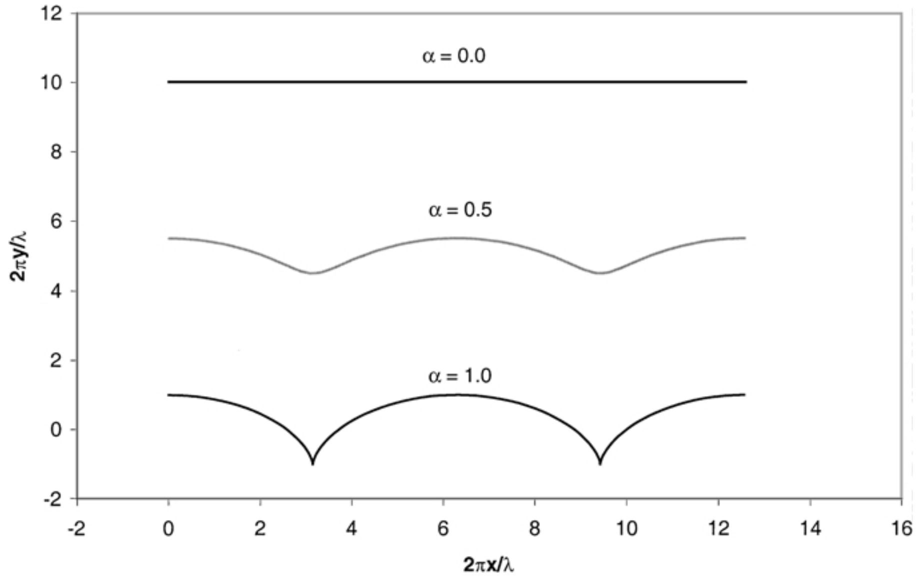

Figure 7. The shapes of the cycloid family: a straight line ($\alpha = 0$), a smooth undulating curve ($0 < \alpha < 1$), a curve with a cusp ($\alpha = 1$).

The interfacial energy is the length of the curved interface times the interfacial energy density:

$$U_{\mathrm{I}} = \gamma R \int_0^{2\pi} (1 + 2\alpha \cos\theta + \alpha^2)^{1/2} d\theta - 2\pi\gamma R. \tag{22}$$

The total free energy is the sum of the above three contributions, and is a function of the generalized coordinates α and β. Denote this function by $G(\alpha, \beta)$. When the generalized coordinates vary by $\delta\alpha$ and $\delta\beta$, the free energy varies by

$$\delta G = -f_\alpha \delta\alpha - f_\beta \delta\beta. \tag{23}$$

The generalized forces are the differential coefficients: $f_\alpha = -\partial G/\partial\alpha$ and $f_\beta = -\partial G/\partial\beta$. A direct calculation gives that

$$f_\alpha = -2\pi\alpha R^2 g + \frac{\pi R^2 \alpha S^2}{E} - \gamma R \int_o^{2\pi} \frac{(\alpha + \cos\theta)\, d\theta}{(1 + 2\alpha\cos\theta + \alpha^2)^{1/2}} \tag{24a}$$

$$f_\beta = -2\pi R^2 g - \frac{\pi R^2 S^2}{E} \tag{24b}$$

The motion of an interface element, δr_n, is linear in $\delta\alpha$ and $\delta\beta$. The differential geometry of the curve gives

$$\delta r_n = N_\alpha \delta\alpha + N_\beta \delta\beta, \tag{25}$$

where the two coefficients are given as

$$N_\alpha = \frac{R(\alpha + \cos\theta)}{(1 + 2\alpha\cos\theta + \alpha^2)^{1/2}}, \quad N_\beta = \frac{R(1 + \alpha\cos\theta)}{(1 + 2\alpha\cos\theta + \alpha^2)^{1/2}} \tag{26}$$

Similarly, the velocity of an interface element is linear in the time rates $\dot{\alpha}$ and $\dot{\beta}$:

$$v_n = N_\alpha \dot{\alpha} + N_\beta \dot{\beta}. \tag{27}$$

The kinetic law (6) can be inverted to express the driving force in terms of the reaction rate, $F = F(v_n)$. The function is given by

$$F(v_n) = \frac{2kT}{\Omega} \sinh^{-1}\left[\frac{v_n}{v_0} \exp\left(\frac{Q - \sigma\varepsilon^*}{kT}\right)\right]. \tag{28}$$

From the elasticity solution in [5] the stress at the interface is given by

$$\sigma = \frac{S(1 - \alpha^2)}{1 + 2\alpha\cos\theta + \alpha^2}. \tag{29}$$

The variational statement (4) becomes

$$\int F(v_n)(N_\alpha \delta\alpha + N_\beta \delta\beta)\, ds = f_\alpha \delta\alpha + f_\beta \delta\beta, \tag{30}$$

where the curve element is given by $ds = R(1 + 2\alpha\cos\theta + \alpha^2)^{1/2}d\theta$. Because $\delta\alpha$ and $\delta\beta$ vary independently, the weak statement (30) results in two equations:

$$\int F(v_n)N_\alpha ds = f_\alpha \tag{31a}$$

$$\int F(v_n)N_\beta ds = f_\beta \tag{31b}$$

Substituting (24)–(29) into (31), we obtain two equations of the form

$$H_\alpha(\alpha, \dot{\alpha}, \dot{\beta}) = 0 \tag{32a}$$

$$H_\beta(\alpha, \dot{\alpha}, \dot{\beta}) = 0 \tag{32b}$$

They are nonlinear, implicit ordinary differential equations for the two functions $\alpha(t)$ and $\beta(t)$. Observe that both equations are independent of β, because a

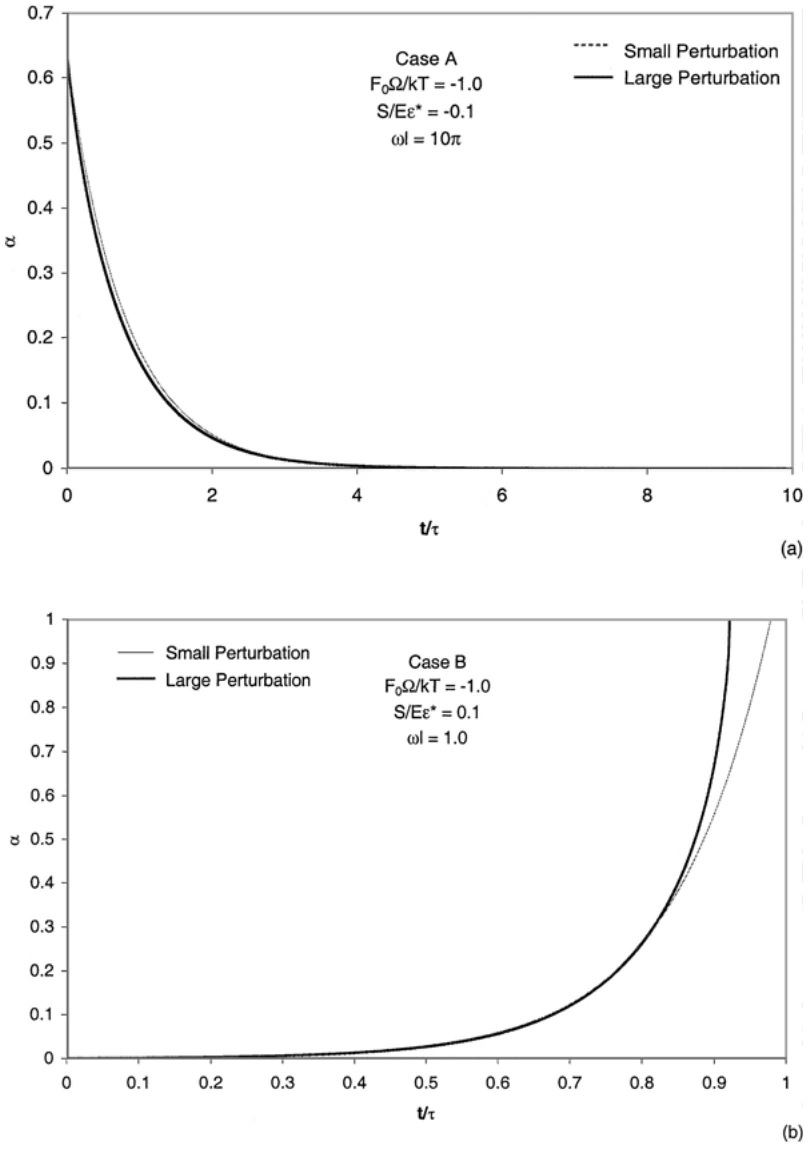

Figure 8. The parameter α as function of time. (a) the initially undulating interface flattens over time. (b) The interface roughens and forms cusps.

translation of the interface does not affect the dynamics. The equations are solved numerically as follows. The values of α and β at $t = 0$ are given. We then find the values of α and β at subsequent times incrementally. At a given time $t = t_i$, the values $\alpha_i = \alpha(t_i)$ and $\beta_i = \beta(t_i)$ are known. Equations (32) are a pair of nonlinear algebraic equations for $\dot{\alpha}$ and $\dot{\beta}$; they are solved by using the Newton-Raphson method. The obtained $\dot{\alpha}$ and $\dot{\beta}$ then update α and β for a small time step.

A dimensionless time is defined as

$$\tau = \frac{t v_0}{\lambda} \exp\left(\frac{-Q}{kT}\right). \tag{33}$$

Figure 8 presents two simulations. The parameters for the two simulations correspond to points A and B in Figs. 5(a) and (b). Case A is from the region where the interface is linearly stable. The nonlinear simulation shows that the interface flattens over time even with a fairly large initial perturbation. In Fig. 8(a), we also plot the result from the small perturbation analysis, taking $\alpha(t) = q(t)/R$. The linear and the nonlinear analysis give very similar results. Case B is from the region where the interface is linearly unstable. The nonlinear simulation shows that the interface will form cusps even when the initial perturbation is very small. Additional nonlinear calculations are performed to determine the condition under which an interface forms cusps. The results are included in Fig. 5(a) and (b) as square dots. The results indicate that linear perturbation analysis gives quite good prediction of crack nucleation.

5. Concluding Remarks

This paper studies the instability of solid-fluid interfaces caused by stress-assisted reaction. We formulate the problem within the framework of partial-equilibrium thermodynamics, in which the solid is in mechanical equilibrium with the applied load, but not in chemical equilibrium with the fluid. The reaction is thermally activated. When the interface is not perfectly flat, the elastic stress in the solid is nonuniform. The stress affects the interfacial reaction through both the driving force and the activation energy. The results of a linear perturbation analysis are discussed in detail, which provide the stability conditions for various parameters. We also present an approximate large perturbation analysis. The results broadly confirm the predictions of the linear stability analysis. It is hoped that further experiments will be carried out to explore the instability under various conditions discussed in this work.

Acknowledgments

This work is supported by the National Science Foundation through grant CMS-9820713.

References

1. W.W. Mullins, J. Appl. Phys. **30**, 77 (1959).
2. D.J. Srolovitz, Acta Metall. **37**, 621 (1989).
3. R.J. Asaro and W.A. Tiller, Metall. Trans. **3**, 1789 (1972).
4. M.A. Grinfel'd, Sov. Phys. Dokl **31**, 831 (1986).
5. C.-H. Chiu and H. Gao, Int. J. Solids Structures **30**, 2981 (1993).
6. K.S. Kim, J.A. Hurtado, and H. Tan, Phys. Rev. Lett **83**, 3872 (1999).
7. W.B. Hillig and R.J. Charles, in *High Strength Materials*, edited by V.F. Zackay (Wiley Inc., New York, 1965), p. 682.
8. T.-J. Chuang and E.R. Fuller, J. Am. Ceram. Soc. **75**, 540 (1992).
9. M.J. Aziz, P.C. Sabin, and G.-Q. Lu, Phys. Rev. B **44**, 9812 (1991).
10. W. Barvosa-Carter, M.J. Aziz, L.J. Gray, and T. Kaplan, Phys. Rev. Lett. **81**, 1445 (1998).
11. Y.G. Shreter, D.V. Tarkhin, S.A. Khorev, and Y.T. Rebane, Phys. Solid State **41**, 1295 (1999).
12. Z. Suo, Advances in Applied Mechanics **33**, 193 (1997).
13. Z. Suo, Int. J. Solids Structures **37**, 367 (2000).
14. C. Herring, in *The Physics of Powder Metallurgy*, edited by W.E. Kingston (McGraw-Hill Book Company, New York, 1951), p. 143.
15. S.P. Timoshenko and J.N. Goodier, *Theory of Elasticity*, 3rd edition (McGraw-Hill Book Co., New York, 1971).
16. H.H. Yu and Z. Suo, J. Appl. Phys. **87**, 1211 (2000).
17. Z. Suo and H. Yu, Acta Mater. **45**, 2235 (1997).
18. H.H. Yu and Z. Suo, Acta Mater. **47**, 77 (1999).